36th Computational Materials Design Workshop
Graduate School of Engineering Science, Osaka University
February 21, 2020

Ternary metal alloy PdRuIr as an effective NO reduction catalyst from first principles analysis

Aspera, Susan Meñez
Nakanishi Laboratory
National Institute of Technology (KOSEN), Akashi College

Introduction: Types of Binary Alloys According to Miscibility

Solid Solution (SS)

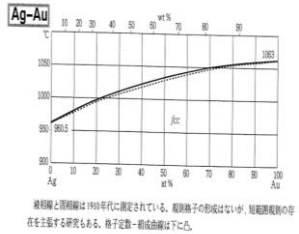

PdAg
AuPd
AuAg

High Temperature Solid Solution (HTSS)

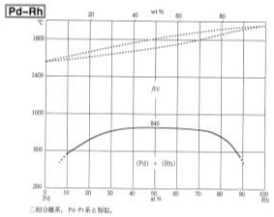

PdRh
PdIr
PdPt

Phase Separation (PS)

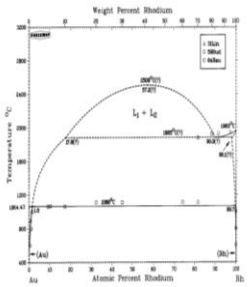

AgRh
AuIr
AuRh

SCIENTIFIC REPORTS

Views: 1,079 Citations: 2 More detail »

Article | OPEN

A Synthetic Pseudo-Rh: NO_x Reduction Activity and Electronic Structure of Pd–Ru Solid-solution Alloy Nanoparticles

Katsutoshi Sato, Hiroyuki Tomonaga, Tomokazu Yamamoto, Syo Matsumura, Nor Diana Binti Zulkifli, Takayoshi Ishimoto, Michihisa Koyama, Kohei Kusada, Hirokazu Kobayashi, Hiroshi Kitagawa & Katsutoshi Nagaoka

Scientific Reports **6**, Article number: 28265 (2016)
doi:10.1038/srep28265

Received: 29 February 2016
Accepted: 02 June 2016
Published online: 24 June 2016

elements is immiscible in the bulk state. Here, we report a Pd–Ru solid-solution-alloy nanoparticle (Pd_xRu_{1-x} NP) catalyst exhibiting better NO_x reduction activity than Rh. Theoretical calculations show that the

AIP | Applied Physics Letters

The valence band structure of Ag_xRh_{1-x} alloy nanoparticles

Anli Yang[1,2], Osami Sakata[1,2,3,a)], Kohei Kusada[2,4], Tomoe Yayama[2,5], Hideki Yoshikawa[6], Takayoshi Ishimoto[2,5], Michihisa Koyama[2,5,7], Hirokazu Kobayashi[2,4] and Hiroshi Kitagawa[2,4,5,8]

+ VIEW AFFILIATIONS

a) Author to whom correspondence should be addressed. Electronic mail: SAKATA.Osami@nims.go.jp.

Appl. Phys. Lett. **105**, 153109 (2014); http://dx.doi.org/10.1063/1.4896857

PREVIOUS ARTICLE | TABLE OF CONTENTS | NEXT ARTICLE

Abstract | Full Text | References (32) | Cited By (8) | Data & Media | Metrics | Related

The valence band (VB) structures of face-centered-cubic Ag-Rh alloy nanoparticles (NPs), which are known to have excellent hydrogen-storage properties, were investigated using bulk-sensitive hard x-ray photoelectron spectroscopy. The observed VB spectra profiles of the Ag-Rh alloy NPs do not resemble simple linear combinations of the VB spectra of Ag and Rh NPs. The observed VB hybridization was qualitatively reproduced via a first-principles calculation. The electronic structure of the $Ag_{0.5}Rh_{0.5}$ alloy NPs near the Fermi edge was strikingly similar to that of Pd NPs, whose superior hydrogen-storage properties are well known.

qualitatively reproduced via a first-principles calculation. The electronic structure of the $Ag_{0.5}Rh_{0.5}$ alloy NPs near the Fermi edge was strikingly similar to that of Pd NPs, whose superior hydrogen-storage properties are well known.

25 Mn	26 Fe	27 Co	28 Ni	29 Cu	30 Zn
43 Tc	44 Ru	45 Rh	46 Pd	47 Ag	48 Cd
75 Re	76 Os	77 Ir		79 Au	80 Hg

25 Mn	26 Fe	27 Co	28 Ni	29 Cu	30 Zn
43 Tc	44 Ru	45 Rh	46 Pd	47 Ag	48 Cd
75 Re	76 Os	77	78 Pt	79 Au	80 Hg

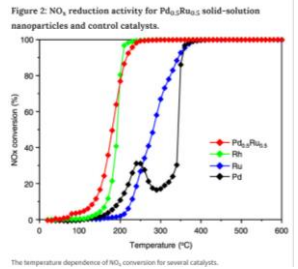

Three-way catalysis of gas exhaust system

Three-way catalytic converter

Reduction of Nitrogen Oxides: $2NO_X \rightarrow x\,O_2 + N_2$ (Rate limiting step)

Oxidation of Carbon Monoxide: $CO + O_2 \rightarrow CO_2$

Oxidation of Hydrocarbons: $C_xH_{2x+2} + [(3x+1)/2]O_2 \rightarrow xCO_2 + (x+1)\,H_2O$

NO reduction activity for PdRu solid solution nanoparticle catalyst

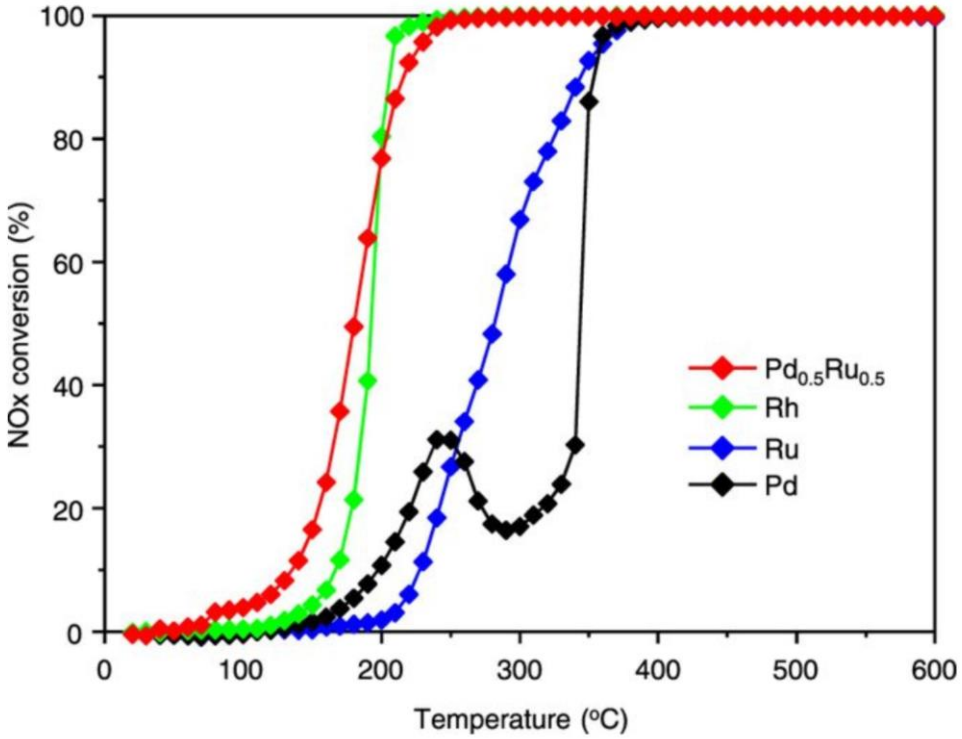

K. Sato *et. al.* , Sci. Rep. - UK **6** (2016) 28265

NO reduction on metal surfaces

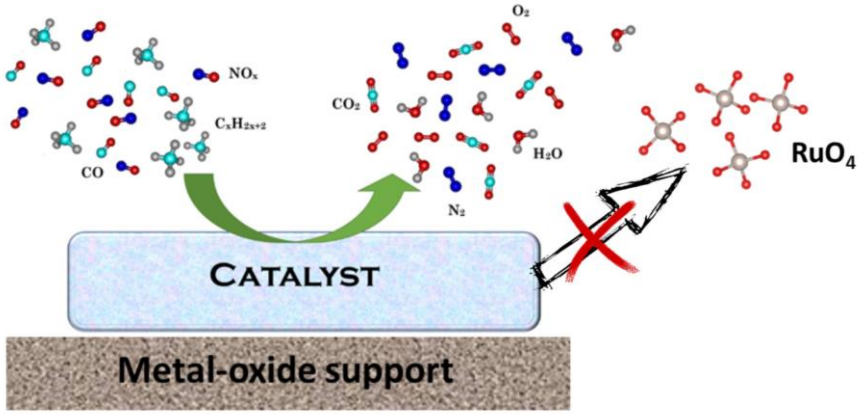

25 Mn	26 Fe	27 Co	28 Ni	29 Cu
43 Tc	44 Ru	45 Rh	46 Pd	47 Ag
75 Re	76 Os	77 Ir	78 Pt	79 Au

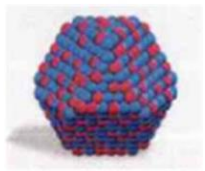

PdRuM-based nano-particle catalyst

NO dissociation on transition metal surfaces

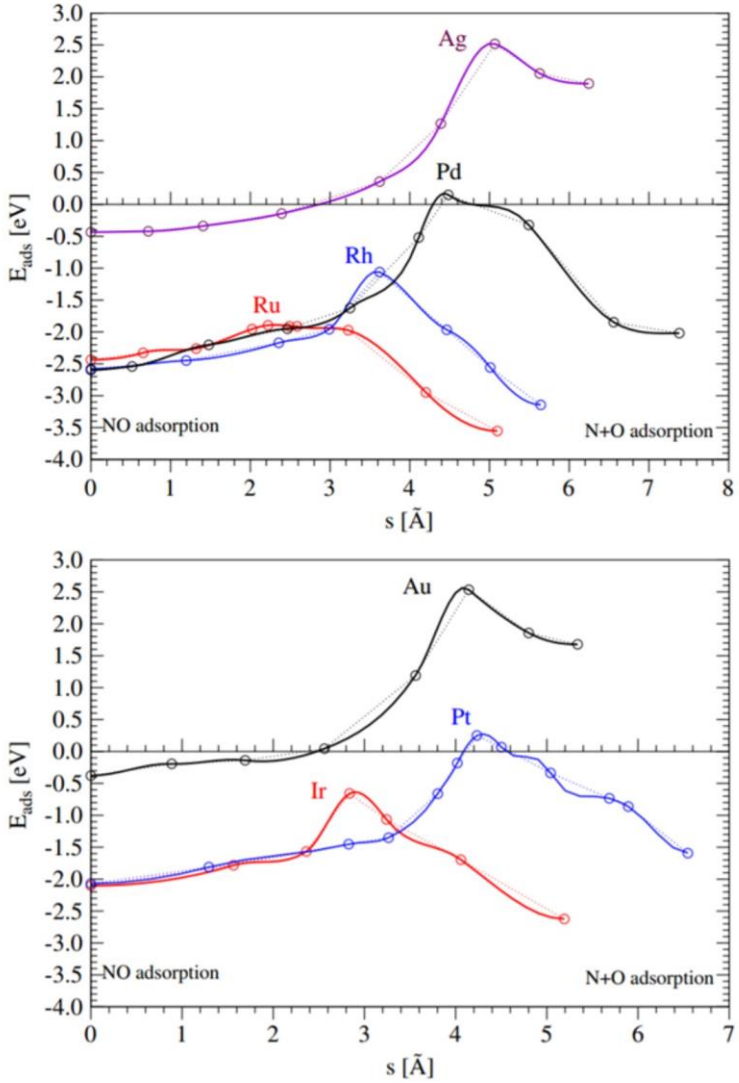

Mechanism of NO reduction on metal surfaces

$$(1)\quad NO + * \rightarrow NO^*$$
$$(2)\quad CO + * \rightarrow CO^*$$
$$(3)\quad NO^* \rightarrow N^* + O^*$$
$$(4)\quad CO^* + O^* \rightarrow CO_2$$
$$(5)\quad N^* + N^* \rightarrow N_2^*$$
$$(6)\quad N_2^* \rightarrow N_2$$

Rate limiting step

Determine the reactivity of PdRuIr alloy catalysts for NO reduction

B. Hammer, J. Catal. **199** (2001) 171.

M. Gadjos, J. Hafner and A. Eichler, J. Phys.: Condens. Matter **18** (2006) 13

Bulk alloy stability

Comparison of bulk formation energy:
Binary vs. Ternary alloy

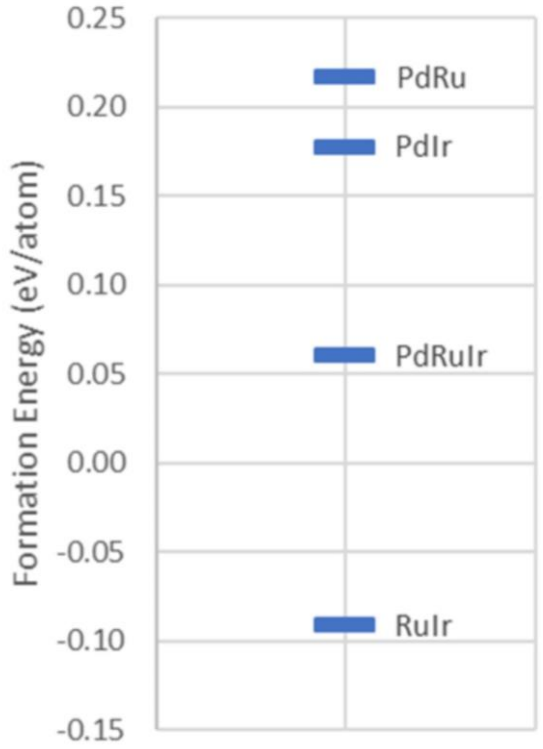

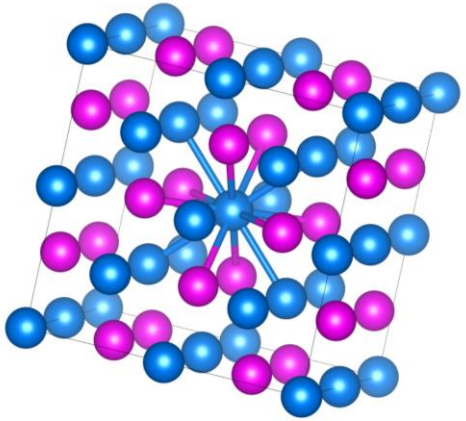

Binary structure

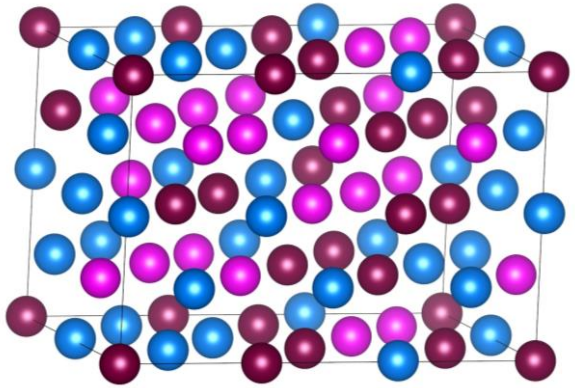

Ternary structure

$$E_{alloying\_bulk} = \left[(N E_{coh\_alloybulk} - \left(\sum (n_i E_{coh\_i}) \right) \right] / N$$

Computational details and model

Computational Details

- Density Functional Theory-based Calculations
- VASP code
- GGA-PBE exchange-correlation functional
- Projector Augmented Wave method for the pseudopotential
- Cut off Energy is 500 eV
- Convergence criteria 1E-5 eV/atom
- 3 x 3 x 5 layers of FCC (111)

Surface Models

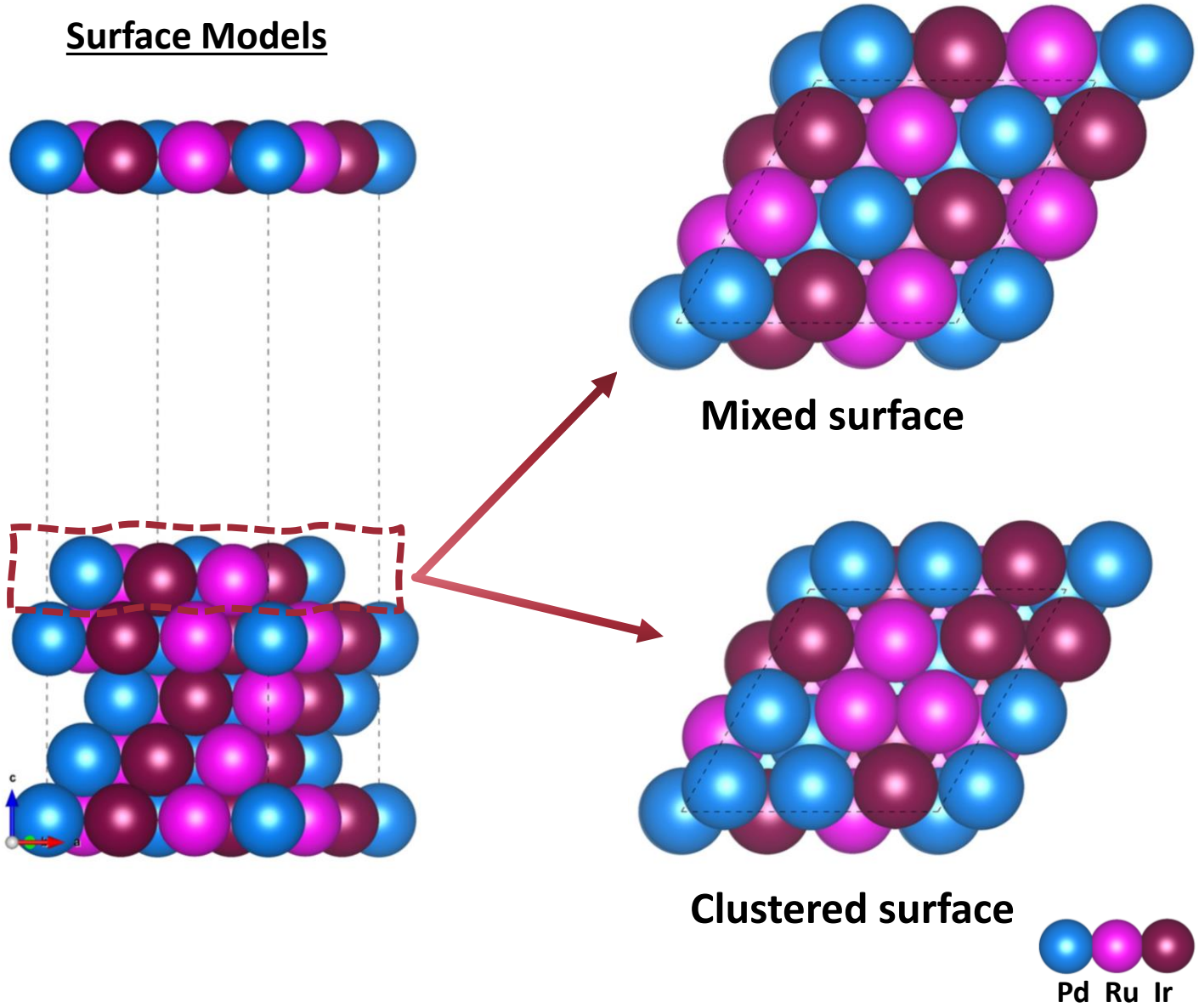

NO adsorption sites

Mixed surface

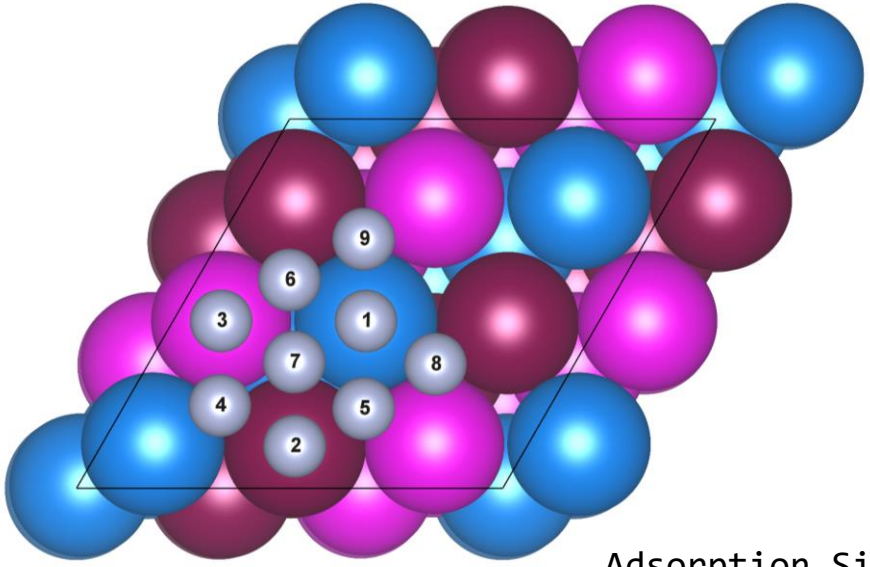

Pd Ru Ir

Adsorption Sites
Top sites
1–top_Pd
2–top_Ir
3-top_Ru

Hollow sites
4–hollow_Pd-Ru-Ir/Pd_fcc
5–hollow_Pd-Ru-Ir/Ir_fcc
6–hollow_Pd-Ru-Ir/Ru_fcc
7–hollow_Pd-Ru-Ir/Pd_hcp
8–hollow_Pd-Ru-Ir/Ir_hcp
9–hollow_Pd-Ru-Ir/Ru_hcp

Clustered surface

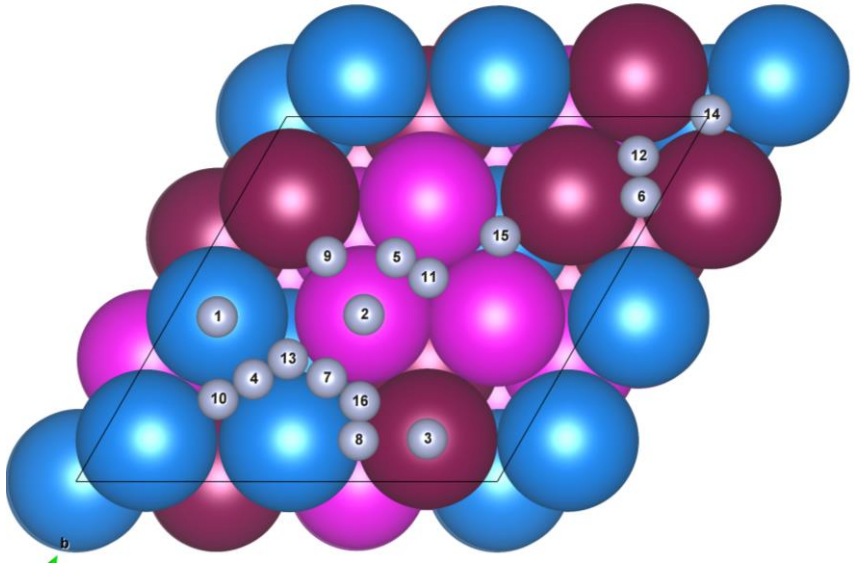

Adsorption Sites

Top sites
1-top_Pd
2-top_Ru
3-top_Ir

Bridge sites
4-bridge_Pd-Pd
5-bridge_Ru-Ru
6-bridge_Ir-Ir
7-bridge_Pd-Ru
8-bridge_Pd-Ir
9-bridge_Ru-Ir

Hollow sites
10-hollow_Pd-Pd-Pd_fcc
11-hollow_Ru-Ru-Ru_fcc
12-hollow_Ir-Ir-Ir_fcc
13-hollow_Pd-Pd-Ru/Pd_hcp
14-hollow_Pd-Ir-Ir/Pd_hcp
15-hollow_Ru-Ru-Ir/Pd_hcp
16-hollow_Pd-Ru-Ir_fcc

NO adsorption on pure surfaces

Reaction path for NO dissociation on pure surfaces

NO dissociation on Rh (111)

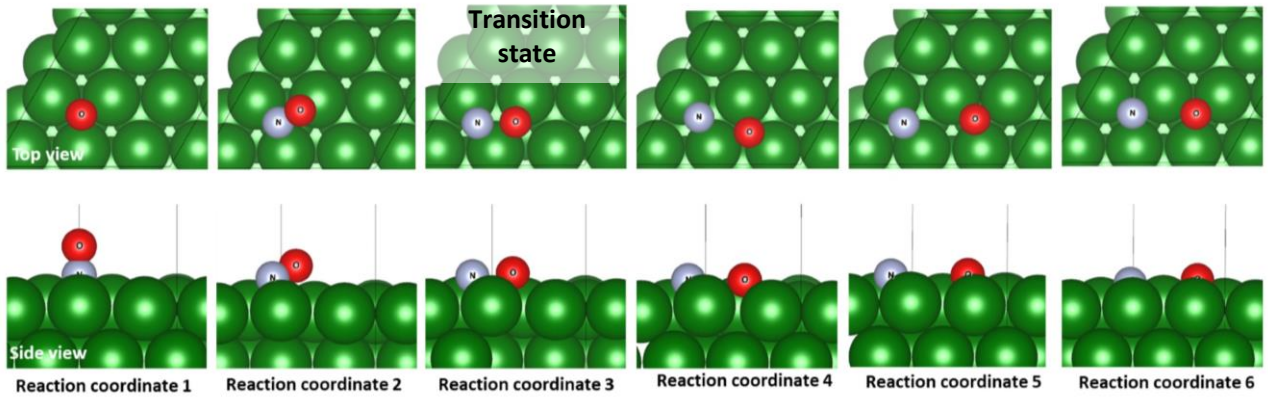

NO charge gain vs. activation energy barrier for dissociation on pure metal surfaces

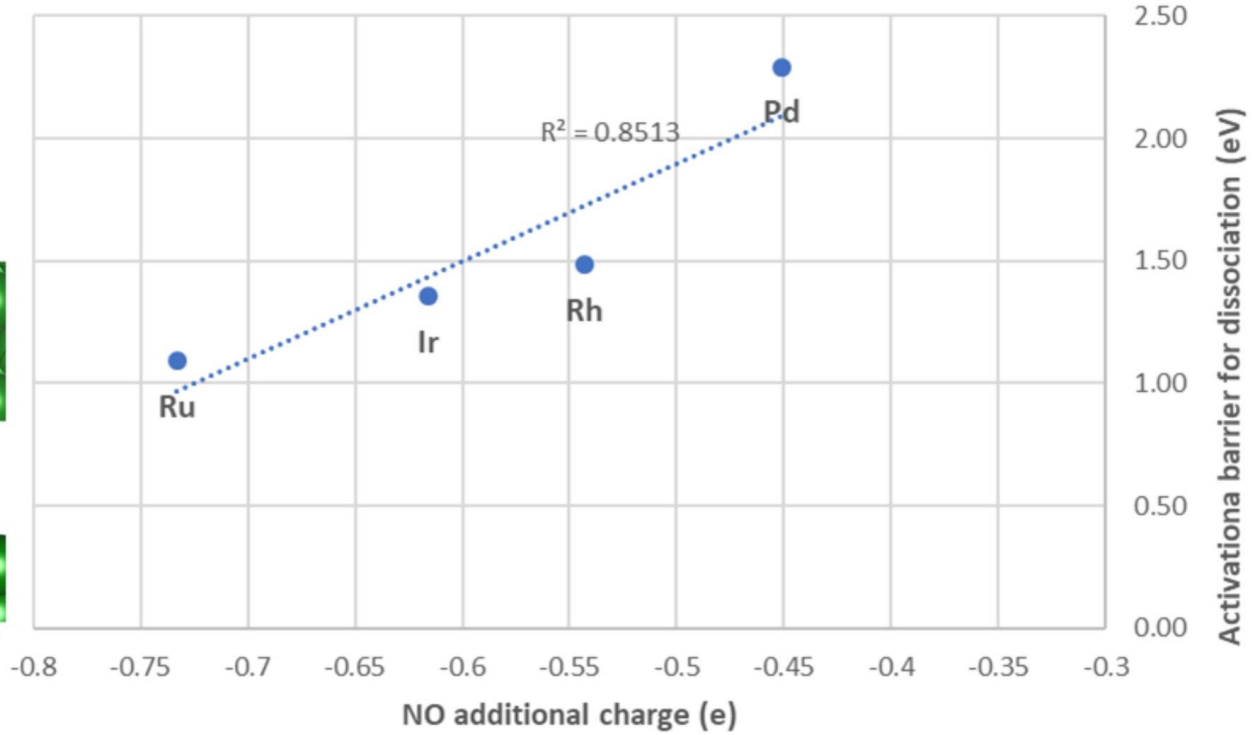

A direct correspondence between NO additional charge and activation energy barrier for dissociation.

Description for Reactivity

NO molecular orbital

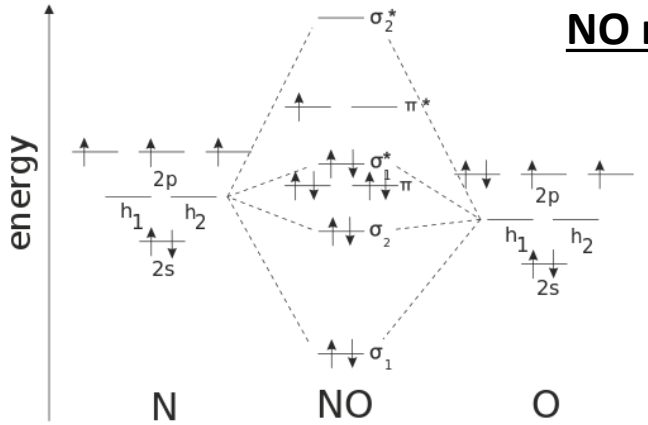

NO adsorption on PdRuIr ternary alloy

Comparison of adsorption energy, N-O bond length and NO additional charge

Initial Adsorption Site	NO adsorption			
	Adsorption Site	Adsorption Energy (eV)	N-O bond length (Å)	NO additional charge (e)
Mixed Surface				
Most stable	Ru top	-2.915	1.18	-0.287
High charge transfer	Ru-Ir/Pd bridge	-2.529	1.22	-0.584
Clustered Surface				
Most stable	Ru top	-2.530	1.18	-0.257
High charge transfer	Ru-Ru-Ir/Pd hcp hollow	-2.523	1.24	-0.674

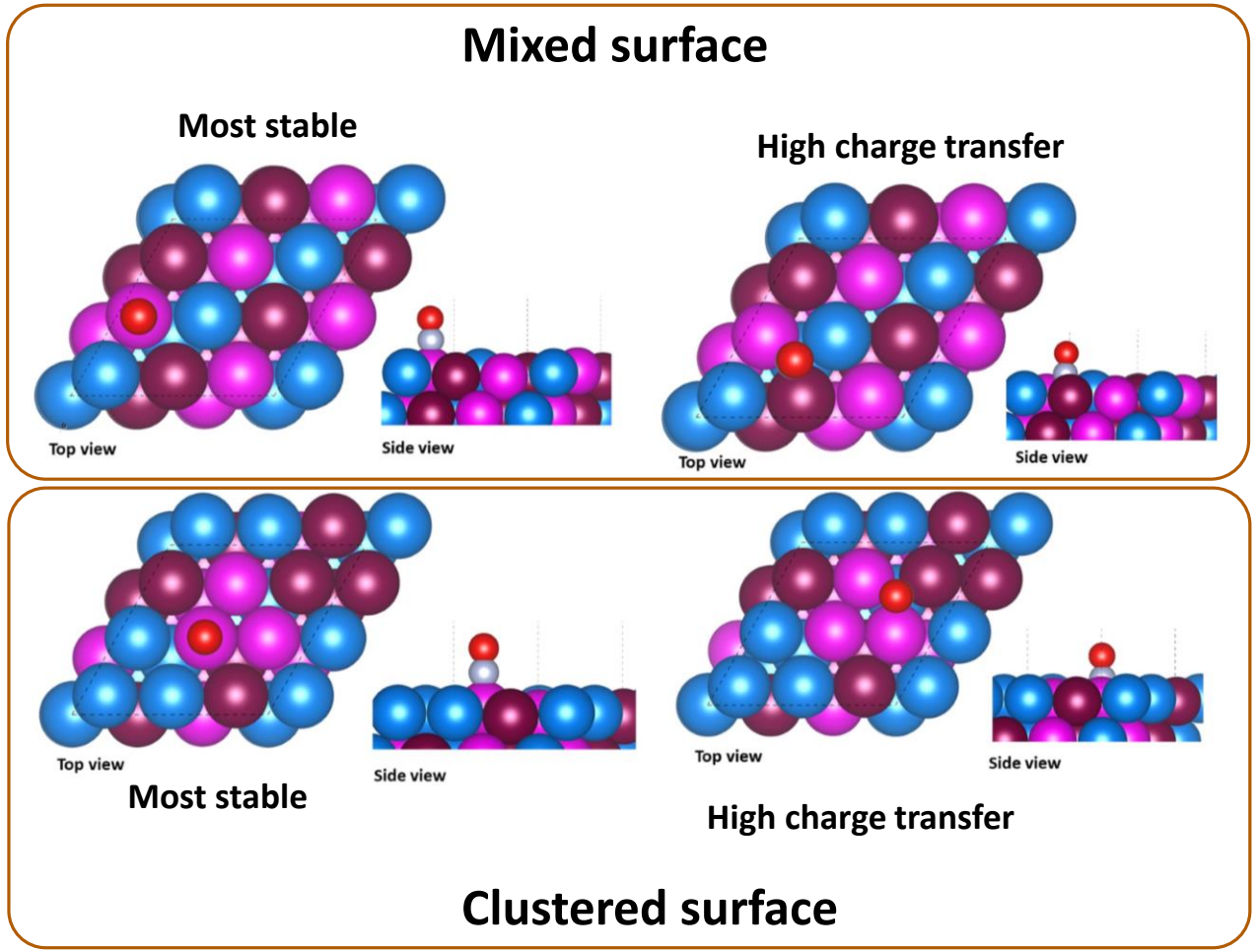

NO dissociation on PdRuIr ternary alloy: from most stable adsorption

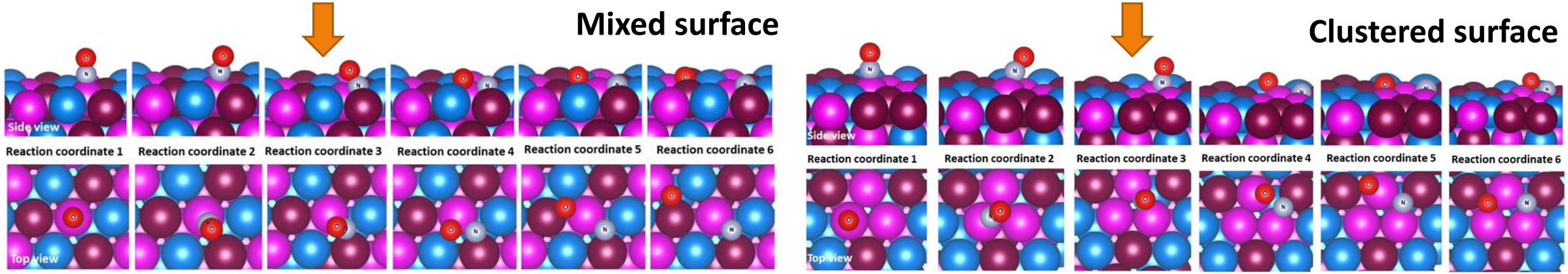

Reaction path for NO dissociation

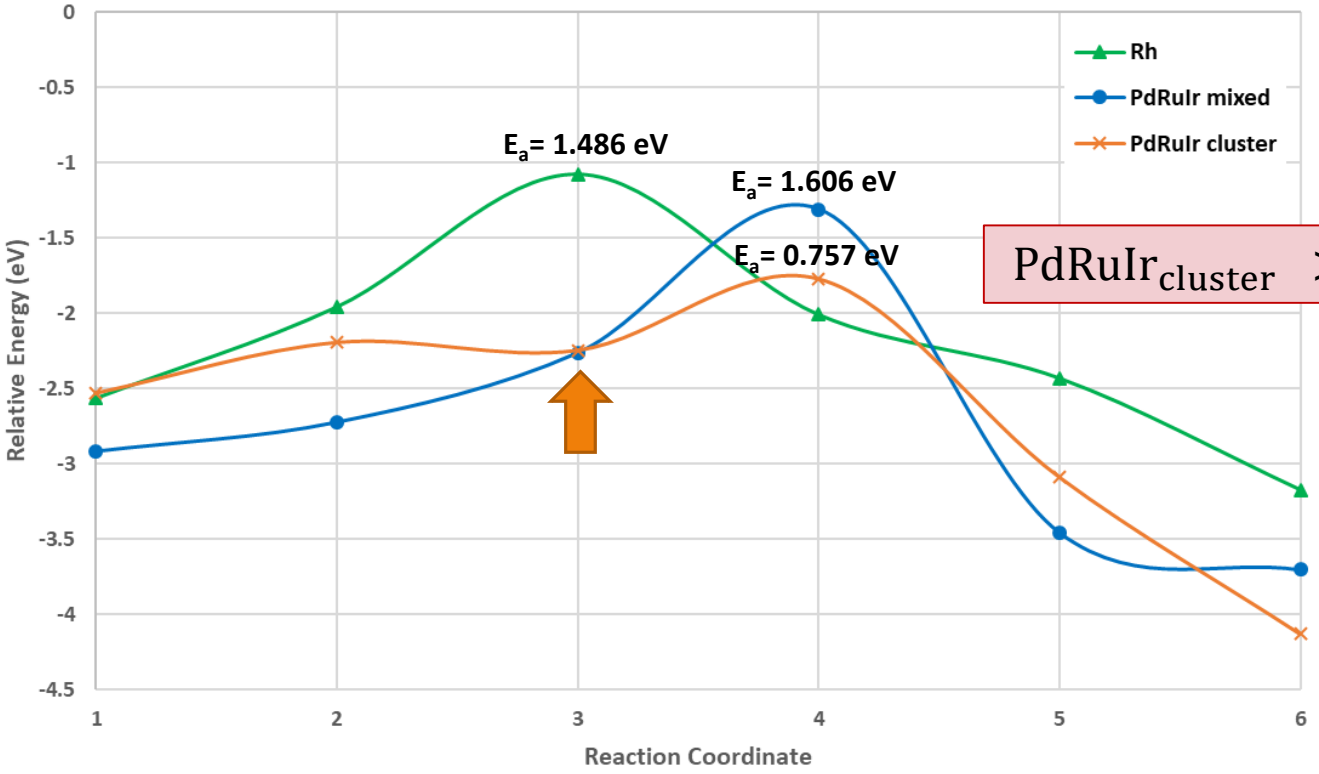

Trend in activity:

$$PdRuIr_{cluster} > Rh\,(111) > PdRuIr_{mixed}$$

Pd Ru Ir

NO diffusion

Reaction path for NO diffusion

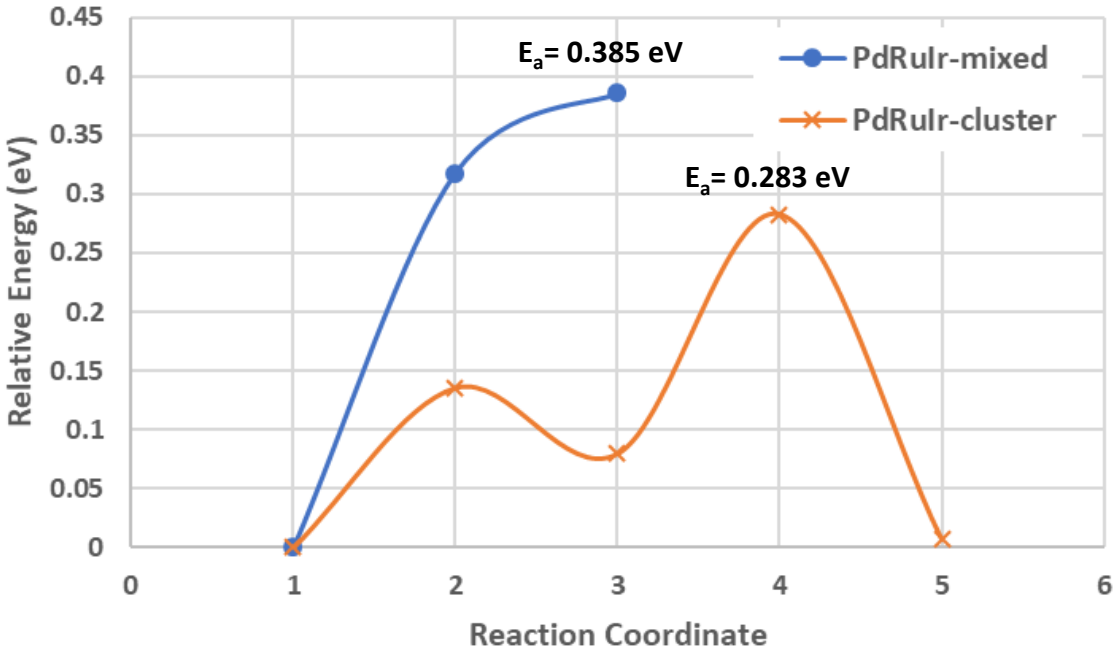

Mixed surface

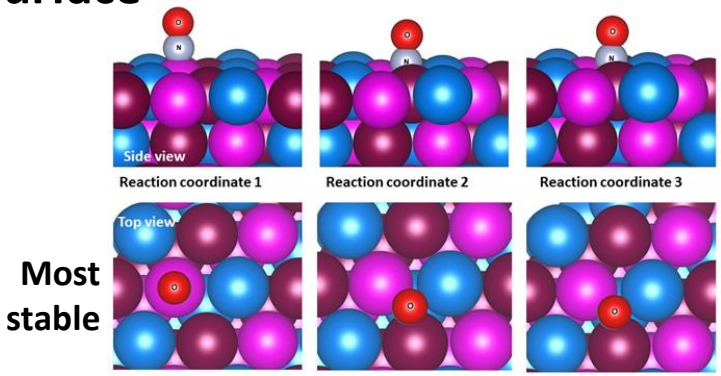

Most stable

High charge transfer

Clustered surface

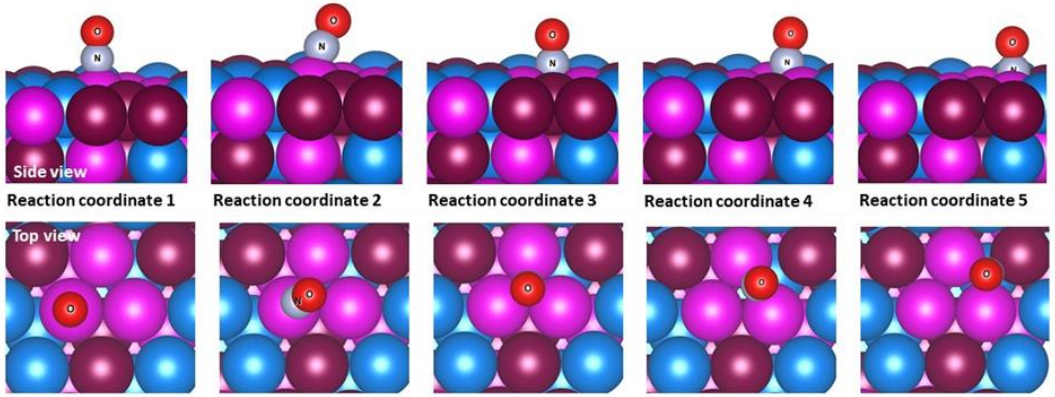

Most stable

High charge transfer

Molecular diffusion on heterogenous surfaces

Most stable adsorption site → Molecular Diffusion → Adsorption site with high charge gain

Active site for dissociation

Pd Ru Ir

NO dissociation on PdRuIr ternary alloy

Reaction path for NO dissociation

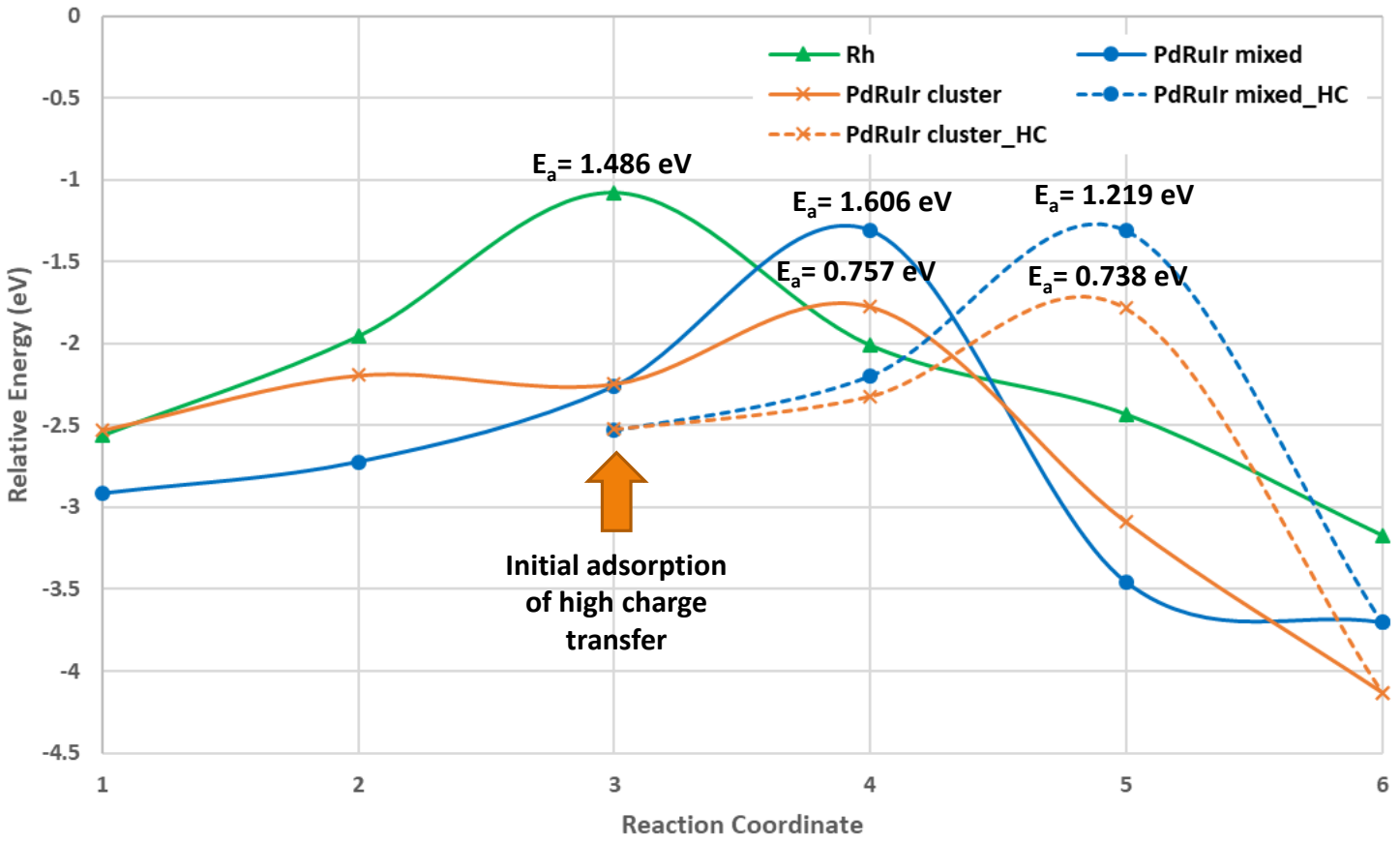

Mixed surface

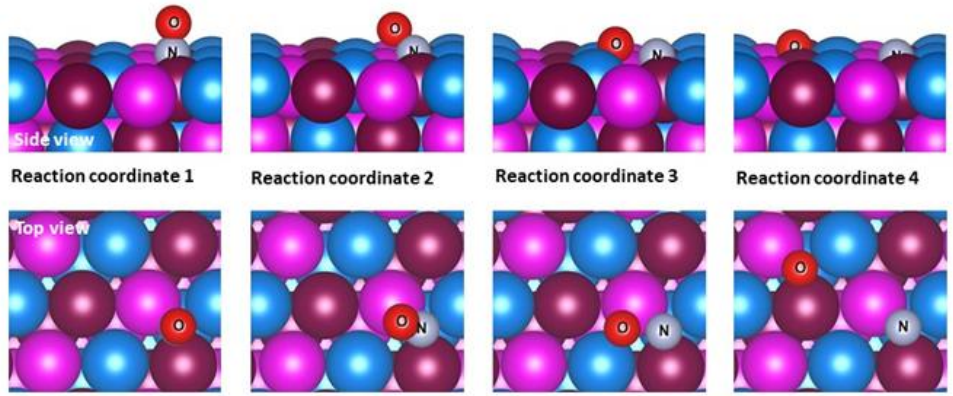

Clustered surface

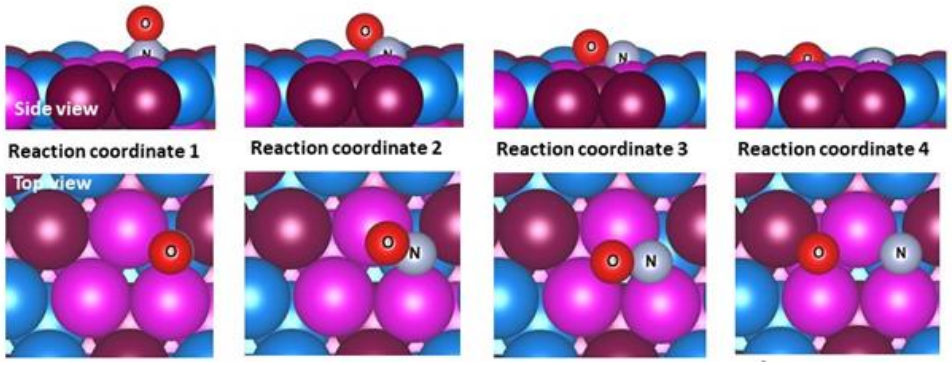

Trend in activity:

$$\mathrm{PdRuIr_{cluster}} > \mathrm{PdRuIr_{mixed}} > \mathrm{Rh\ (111)}$$

Pd Ru Ir

Electronic properties

Local density of states

Mixed surface

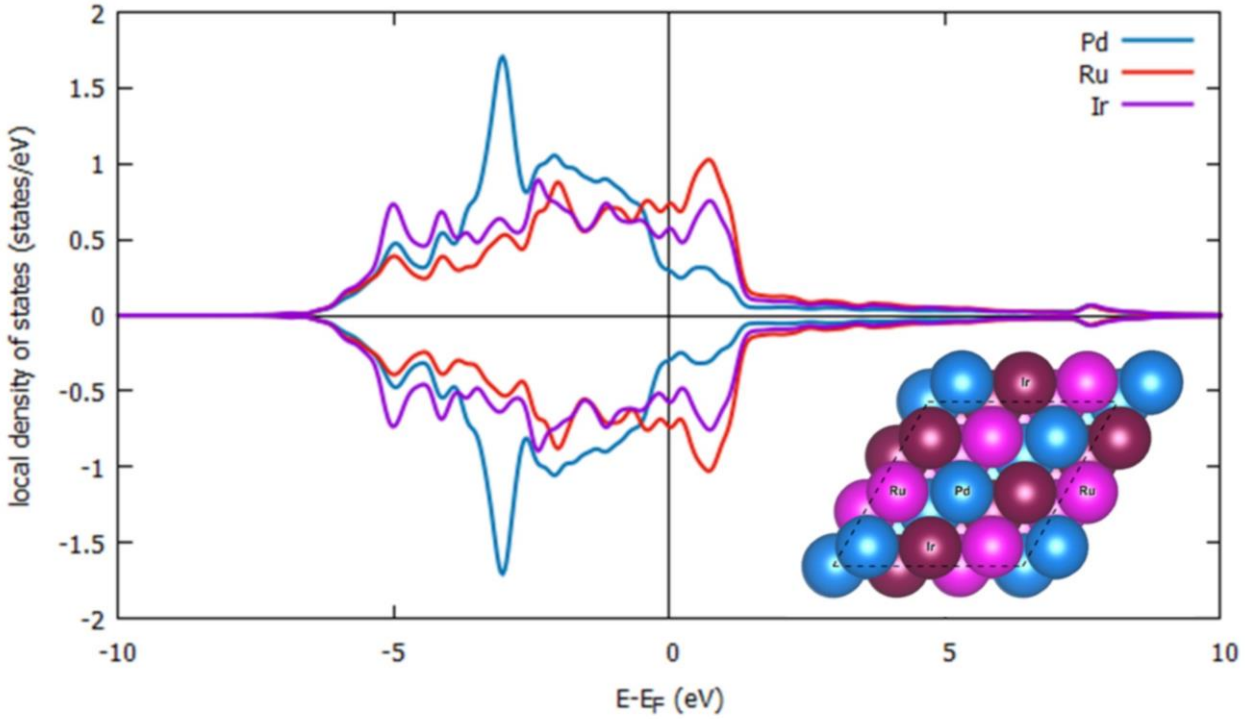

Clustered surface

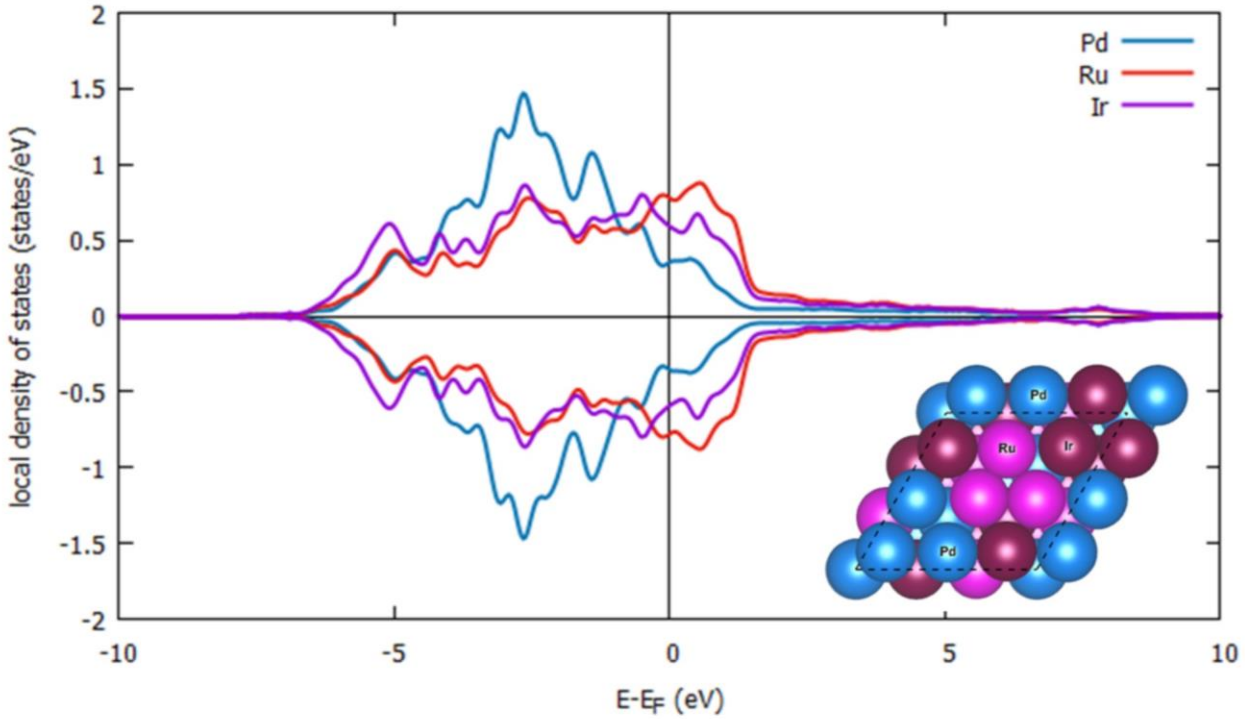

O adsorption on ternary PdRuIr

Comparison of O adsorption energy and O addition charge

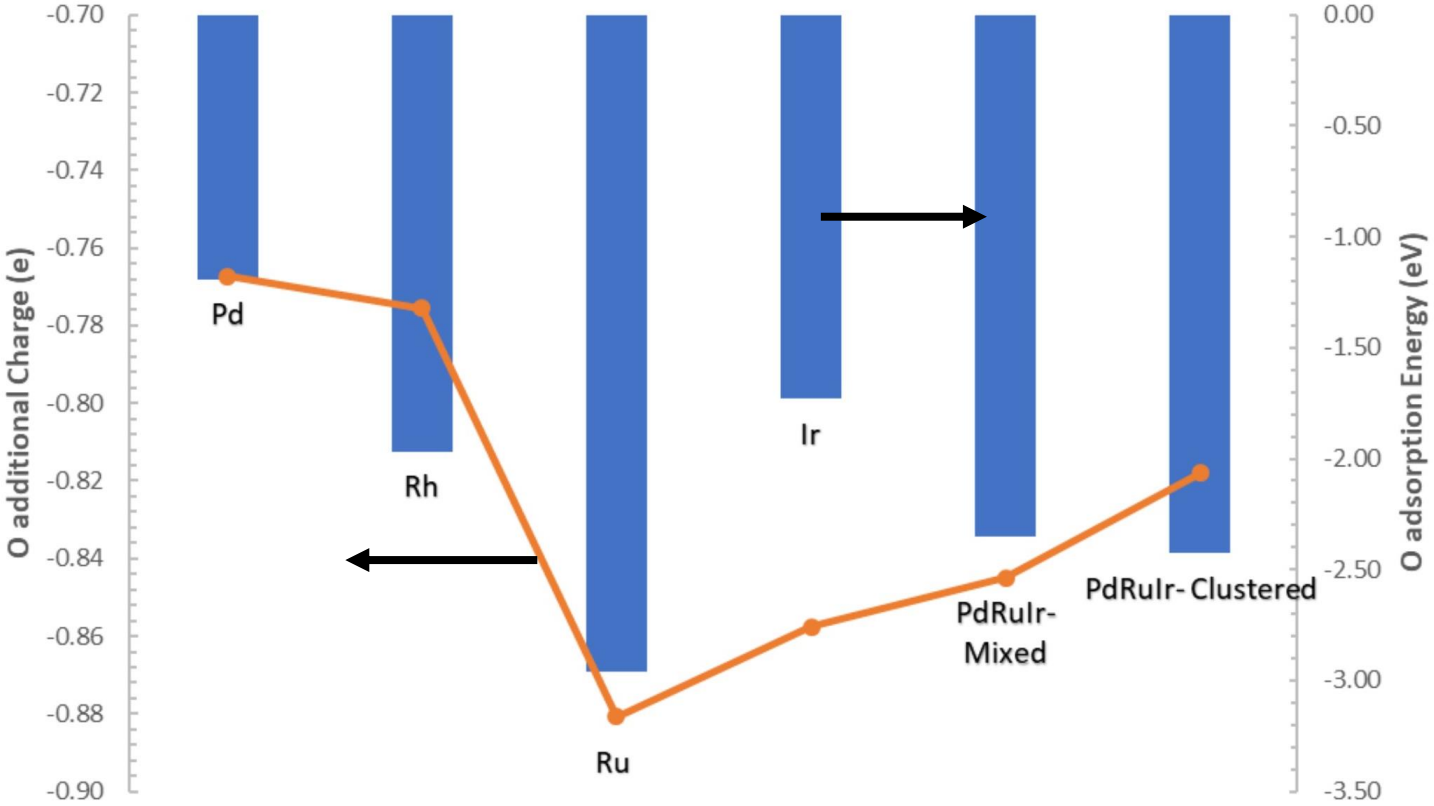

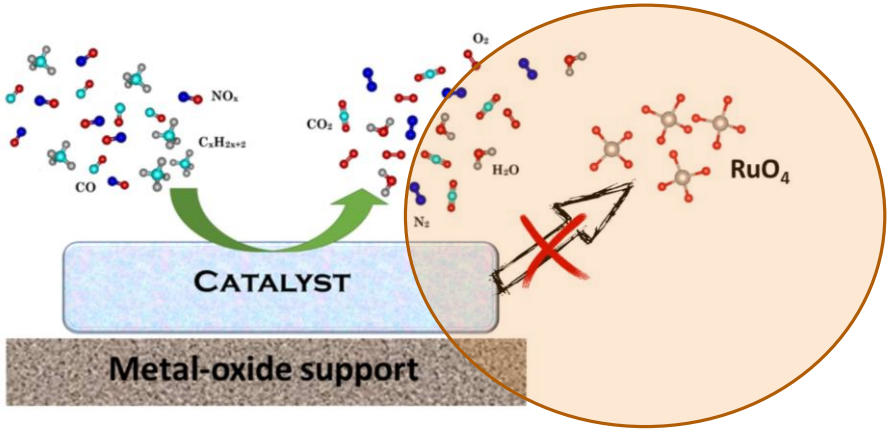

Mixed surface

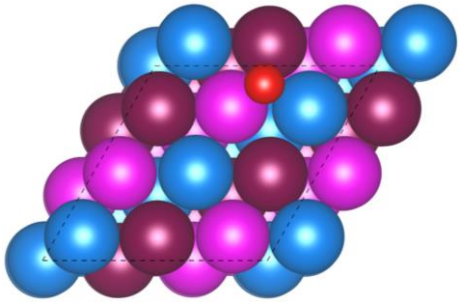

Clustered surface

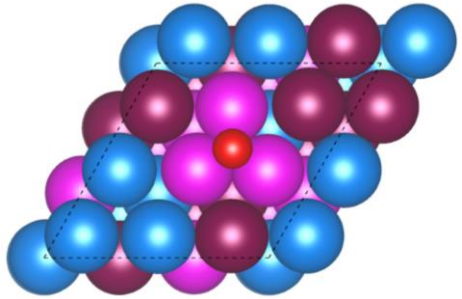

Bader charge analysis

Charge re-distribution due to alloying

Surface Atoms	Effective Charge (e)		
	Mixed Surface	Clustered Surface	
Pd	-0.079	-0.080	gain
Ir	-0.222	-0.188	gain
Ru	0.161	0.138	loose

*Effective charge is relative to the valence electron number of the isolated atom, negative (-) value entails gain of electron and positive (+) value entails lost of electron.

Change in atomic charge after NO adsorption

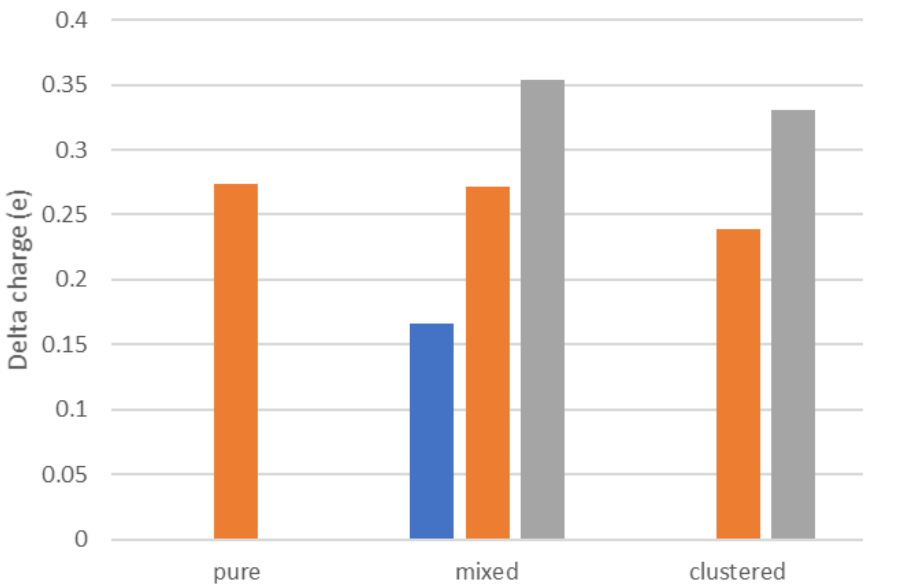

Mixed surface

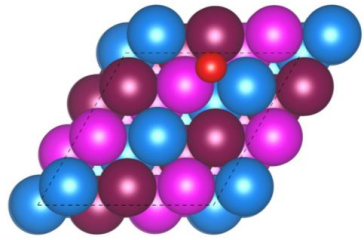

Clustered surface

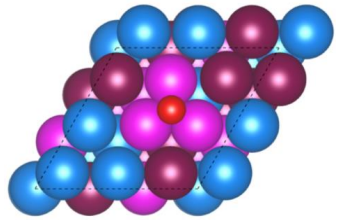

Summary

- The reactivity for NO reduction on **the PdRuIr ternary alloy** was analyzed using first principles calculation based on density functional theory. Two surface surfaces of different atomic configuration was considered: (1) mixed ordered surfaces and (2) local clustering of surface atoms.
- Analysis of NO dissociation path shows that the **mechanism in heterogenous alloyed surfaces could follow a different path than pure surfaces**, i.e., NO dissociation on alloyed surfaces could be initiated by molecular diffusion on an active site.
- With that, most stable NO adsorption may not determine activity, rather **additional charge gain** by NO upon adsorption at the surface could be an indication of activity.
- For the ternary alloy PdRuIr, **activation energy barrier is lower** on a **PdRuIr ternary alloy** than the Rh (111) surface.
- Ternary metal alloying altered the surface charge distribution such that **Ru surface atoms** are **partially oxidized**. With this, **oxidation by adsorbate O atoms will be less probable**.

Acknowledgement

- JST ACCEL Program --- (JPMJAC1501) "Creation of the Functional Materials in the Basis of the Inter-Element-Fusion Strategy and their Innovative Applications"
- JST CREST--- (No. 17942262) "Innovative Catalyst and Creation Technologies for the Utilization of Diverse Natural Carbon Resources: In-situ Atomic Characterization of Catalytic Reactions for the Development of Innovative Catalysts"

NAKANISHI LABORATORY

Thank you very much.
どもありがとうございました。